Chapter 2

New Developments on Mini/Micro Shape Memory Actuators

Adelaide Nespoli, Carlo Alberto Biffi, Riccardo Casati, Francesca Passaretti, Ausonio Tuissi and Elena Villa

Additional information is available at the end of the chapter

http://dx.doi.org/10.5772/50473

1. Introduction

Shape Memory Alloys (SMAs) are functional materials, characterized by some attractive features, such as pseudo-elasticity (PE) and shape memory effect (SME) [1]. The latter consist in the capability of the material to recover high deformation values by heating and can be considered very suitable for actuation applications.

In the actuation field, the most common shape memory alloy is quasi-equiatomic NiTi system, commercially known as Nitinol®. Ti-rich NiTi compounds show characteristic transformation temperatures higher than the room one and they can recover high values of deformation. Moreover, these intermetallic compounds are widely used since they exhibit high thermal and mechanical cycling stability. Other NiTi-based alloys are also employed for this kind of applications. In particular, NiTiCu, with Cu substituting Ni in the 3-10at% range, or NiTiCo system are used respectively when the application requires narrow thermal hysteresis or high stiffness.

In Figure 1, the comparison between differential scanning calorimetry (DSC) data derived from NiTi wire (200 μm in diameter) in fully annealed condition and after aging (500ºC for 10 minutes) are reported. As it can be seen, the fully annealed NiTi alloy goes into a one-step transformation both during cooling and heating. In this case, shape memory effect occurs by a martensitic transformation (MT) between a low-temperature monoclinic structure, B19’, called martensite, and a high-temperature body-centered cubic parent phase, B2, called austenite. When the material is aged at specific temperatures, this transition may occur in two steps in association with a trigonal phase, called R-phase [1].

During heating, the phase transformation, named inverse MT, is defined by austenitic start (As) and finish (Af) temperatures. Similarly, during cooling direct MT is defined by martensitic start (Ms) and finish (Mf) temperatures, respectively.

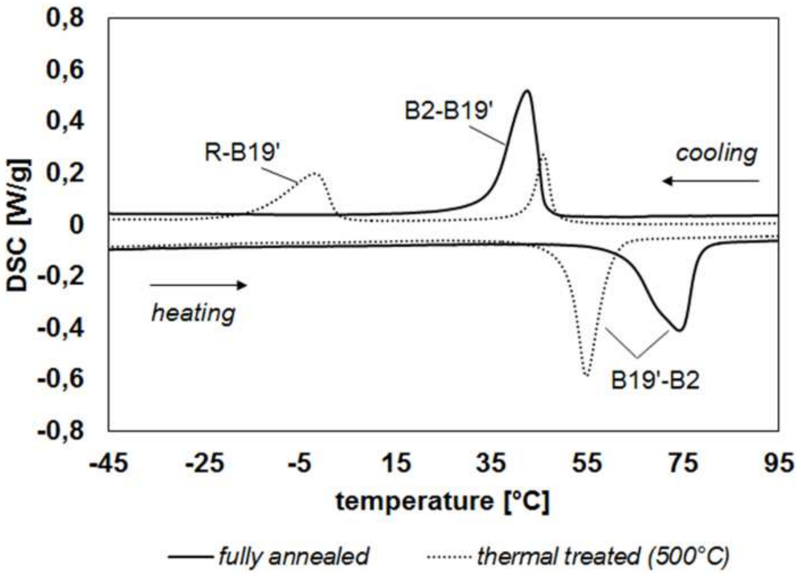

Figure 1. DSC scan of 200μm NiTi wire in the fully annealed state and after aging (500°C for 10 minutes).

Then, the deformation induced by a state of stress on a SMA element can be recovered heating the material over the austenitic characteristic temperatures: the shape recovery starts at As and finishes at Af.

The transition temperatures are strongly influenced by the applied load, since it stabilizes the martensitic structure causing an increase of all transition temperatures. This behavior of SMA is well described by the Clausius-Clapeyron law [1-5].

Furthermore, SMA actuators generally need a training to stabilize their fatigue properties in terms of transformation temperatures and strain recovery. For example, a possible procedure consists in the thermal cycling under a constant load. Figure 2 depicts the evolution of the temperature-stroke relationship during the first thermo-mechanical cycles. It is seen that the stabilization of the material behavior can be reached after few thermal loops.

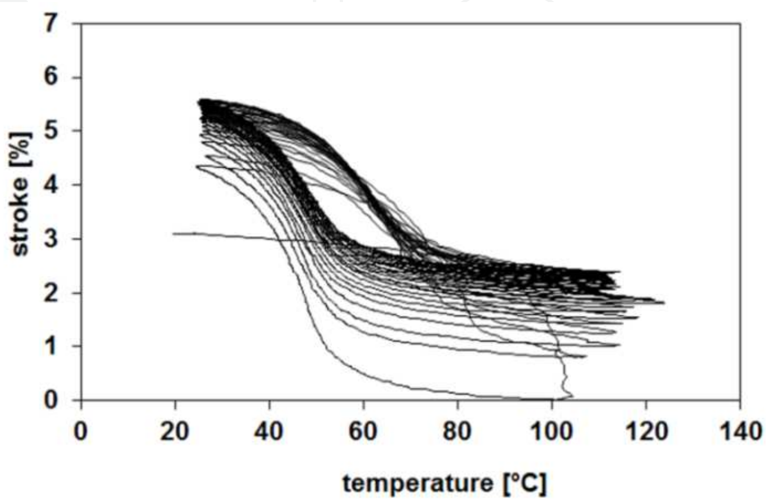

Figure 2. Example of thermo-mechanical hysteresis typical of a SMA material.

Since SMA can generate mechanical work, they are employed as actuators. The functional properties of SMA element used in actuators strictly depend on several factors, such as the chemical composition and the thermo-mechanical history[1,4,5].

Nowadays, the tendency is to produce ever smaller actuators because of the continued miniaturization of all the industrial products. In general, a mini-actuator may be composed by only a SMA element or by a mini-modular device, in which the SMA element is embedded and acts as the core and active part.

In this chapter, the fundamental operating parameters, which affect the performance of shape memory thin wires, are reviewed. Then, the influence of electrical heating conditions performed by different waveforms on functional fatigue of NiTi micro-wires is also reported.

When the SMA element is embedded into a mini-modular mechanical device, its shape could be a serious problem as spaces are very restricted. To solve this drawbacks, a new SMA conformation suitable for the mini and micro scales is presented: it consists of a planar wavy formed NiTi wire, called snake-like arrangement. Currently, this configuration of the SMA wire is principally exploited in the textile and medical domains [6-8]. n the micro scale, original works are reported by Mineta et al. [7-8], who produced different SMA snake elements by means of electrochemical etching for obtaining bending motion of active catheters. Khol et al. [9] used the micro snake geometry to activate a microgripper system. Moreover, Leester-Schadel et al. [10] adopted laser technology to produce micro SMA snake actuators and then used the batch fabrication process to obtain more articulated samples. In this chapter the main mechanical performance of this unusual geometry and its exploitation in a mini-modular mechanical device are presented.

Another topic of this work is related to a current research on fabrication and characterization of SMA micro-snakes, by means of laser technology and following polishing processes. The reason why this non-traditional production technology has been chosen for this purpose is due to its flexibility in the machining of small features, high productivity and repeatability [11-12]. Considering the direction of miniaturization of the products during the recent years [13], in the last part of the chapter the rescaling of SMA mini-snakes down to micro-scale is presented. The attention is also focused on the evaluation of the capability of laser micro-cutting industrial process in the fabrication of micro-snakes from NiTi SMA sheets [14-17]. The evaluation of the thermo-mechanical properties of the produced actuator in correspondence of the different fabrications steps is then presented and discussed in order to describe the behavior of the micro-snake-like element for actuation.

2. SMA linear actuators

The first case study is the application of a simple straight wire as base element for actuation systems [18]. The most important functional properties, which characterize shape memory wire for actuators, are the capability to recover high strain values, the characteristic transformation temperatures and the thermo-mechanical cycling stability [1]. These characteristics of SMA can be tailored acting on chemical composition, thermal and mechanical processing, shape setting treatment and training [1, 20-25].

In recent years, the good ductility of NiTi intermetallic has been exploited for the production of few tens micron wires [21, 26, 27].

Thanks to their small dimensions, such thin wires permit to reach very short cooling time but, obviously, they can be employed just in all those applications in which high loads are not required. The fabrication of these products has led to the miniaturization of SMA components for actuators that are nowadays employed for new kind of devices such as optical image stabilizer and autofocus for small camera [26]

During working life, the SMA wire is subjected to thermo-mechanical cycling and accumulates plastic deformation, elongating irreversibly and reducing its diameter (see Figure 3). This behavior has to be considered in actuator design. Another important point to consider is the unsteadiness of the functional properties of shape memory wires during the working life. The plastic deformation induced during the thermo-mechanical cycling leads to a change of microstructure of SMA wire. Lattice defects, dislocations and nano-scaled precipitates are introduced into the matrix and they cause significant changes in transformation temperature and in the capability of the material to recover a deformation [28-30], as depicted in Figure 4.

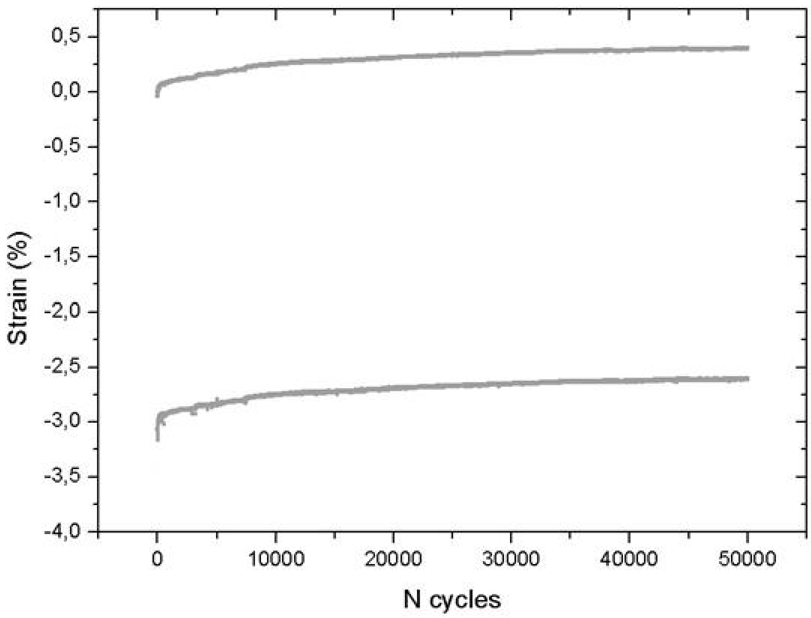

Figure 3. Thermal cycling of a 80μm wire under constant stress (200MPa). The heating was performed by electrical pulse, and stroke was limited at 3%.

In most cases, SMA wires used as actuator, are heated by means of an electrical pulse (Joule effect) and cooled by natural air convection. So, it is very easy to reach short actuation time (heating time) but the reset time (cooling time) cannot be substantially controlled. Slight improvement in the reduction of reset time is achieved positioning the shape memory wire horizontally [19], as shown in Figure 5. In this figure, it can be noticed that after heating (at

200s) the strain is maintained to two constant values for both the two configurations till time is near to 230s and 250s for horizontal and vertical position respectively. After these points, the two wires start the cooling process which results to be faster for the horizontally positioned wire than the vertical one. As an example, it can be seen that at 275s the horizontally positioned wire recovers half of its maximum strain while at the same time the vertical positioned wire has just started the cooling route.

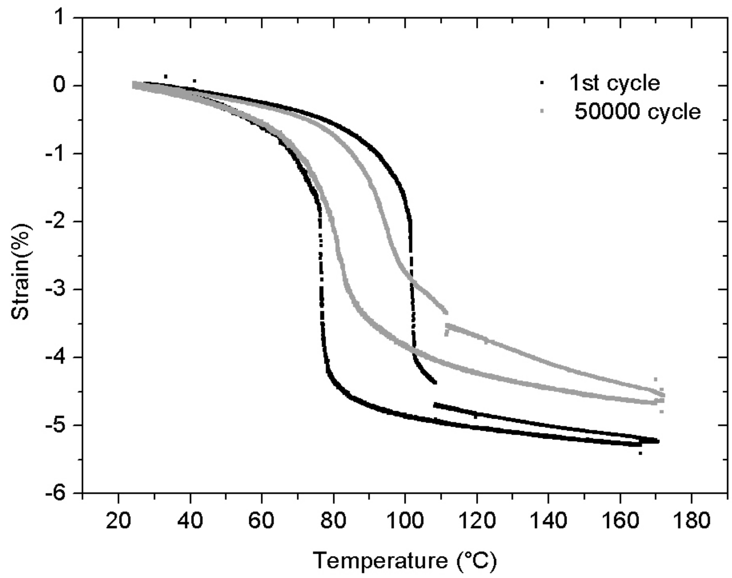

Figure 4. Thermal loop under constant stress (200MPa). The heating was performed by a thermal chamber. The test was carried out on a 80μm wire before and after $5x10^4$ thermal cycles under constant stress (200MPa).

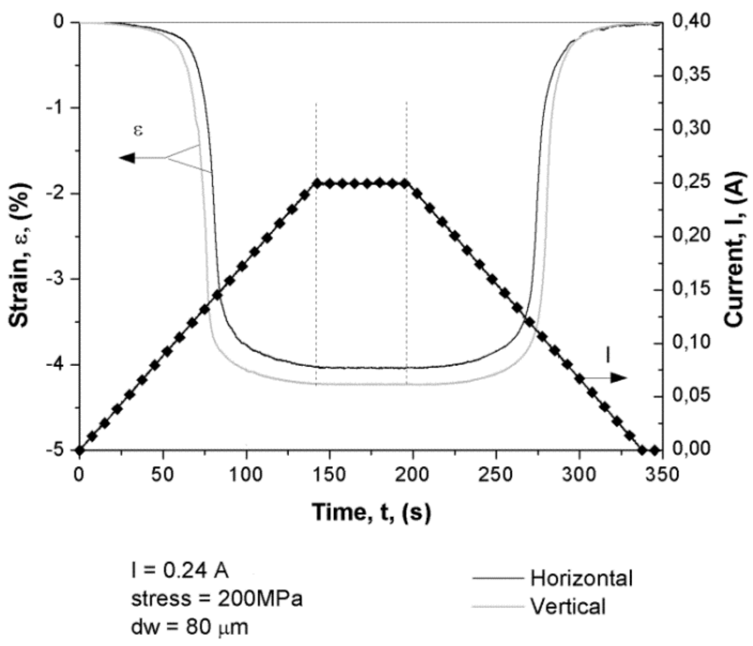

Figure 5. Comparison between the mechanical performance of horizontal and vertical configuration of 80μm SMA wire used as actuator [19].

As previously stated, the heating process of a SMA actuator can be easily obtained by Joule effect. In this case, it has to be considered that the shape of the electrical pulse used for the actuation strongly affects the functional properties of SMA [27]. As an example, Figure 6 shows the time required by the wires to recover the 3% of deformation (actuation time) when it is heated by two different current pulses. At the 1st cycle ramp and step electrical pulse employed to heat two 80µm wires were designed to have the same electrical efficiency but the actuation time is 400ms by step current pulse while it is 623ms by ramp. After $5{\cdot}10^3$ cycles the wire heated by step pulse employs 618ms, so 218ms more than the time employed at the first cycle. As opposite, the ramp pulse leads to an increase of just 22ms. After $5{\cdot}10^4$ cycles the actuation time related to the wire heated by step is even higher than the one related to wire heated by ramp. This behavior leads to a drastic decrease of the step heating method efficiency (from 0.91% to 0.55%), vice versa the efficiency of the ramp heating method does not change so much (from 0.91% to 0.75%).

Then, in order to achieve fatigue performance acceptable for the specific device, the right electrical pulse has to be chosen considering the number of cycles that the SMA actuator has been designed to work.

Recently, the effect of drawing procedure on functional fatigue of thin NiTi wires has also been investigated [21]. Basically, 80µm NiTi wires were produced through two different drawing procedures reaching the same final cold working level before shape setting. These two processes differ for the number of drawing steps carried out to reach a certain cold working level before each heat treatment. After the last thermal treatment the specimen that underwent to a less number of drawing steps shows a narrow thermal hysteresis, even after thermo-mechanical cycling (see Figure 7). It means that adopting a severe drawing procedure leads to improve the actuation performance.

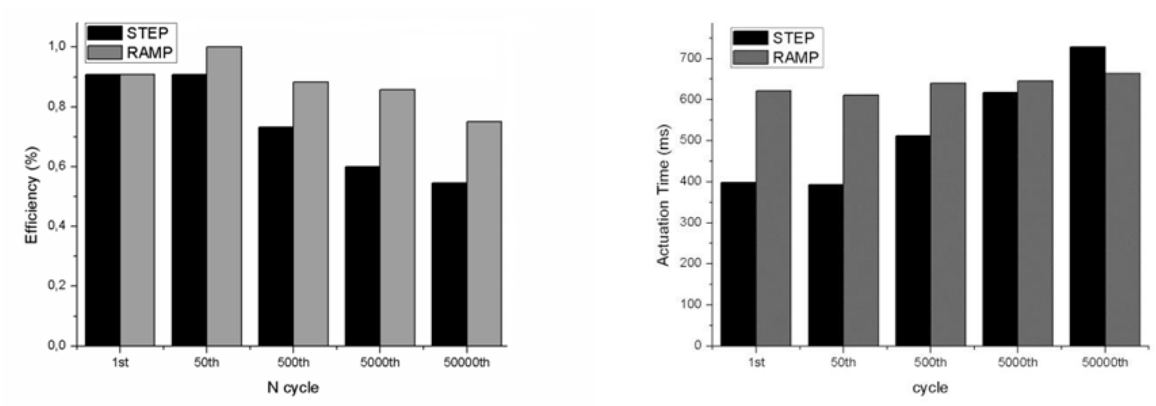

Figure 6. Actuation time tests performed by electrical heating (on the left) and by efficiencies (on the right).

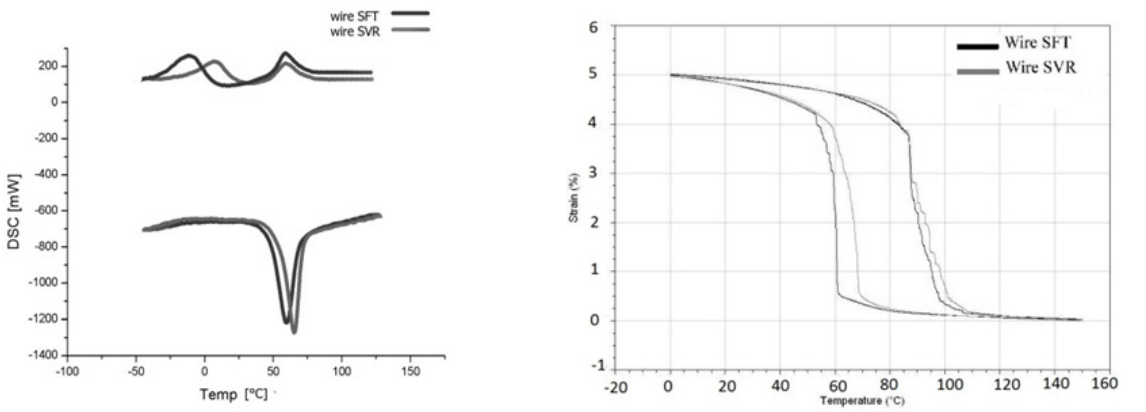

Figure 7. DSC scans, on the left, and thermal loop under constant tensile stress, on the right, of two 80μm NiTi wires obtained by a severe (SVR) and soft (SFT) drawing procedure.

3. Snake-like SMA actuators

The main focus of miniaturization is to develop devices with high mechanical performance in very limited spaces. In the SMA field, the mini-actuator may be composed by only the SMA element or by a mini-modular device in which the SMA element is embedded and acts as the core part. In the latter case, some issues typical of SMA miniaturization should be taken into a serious consideration: first of all, the fixing points of the SMA element and the electrical contacts should be adequately designed to prevent abrupt rupture, and then the use of a wire geometry generally implies the employment of additional mechanical parts which may affect the long run performance of the SMA element.

The mechanical work resulting from the SMA shape recovery is used to produce linear or rotational motion in smart actuators. To attain high strokes in limited space, designers developed several miniature devices which include SMA elements with a straight or a helical spring shape [31]. These two shapes present two opposite mechanical behaviors: the straight conformation allows high forces but smart wire arrangements should be employed in order to achieve also high strokes. As an example, Jansen et al. used two sets of seven pulleys to arrange a 1000mm long SMA wire with a diameter of 0.200mm, and attain 3% of stroke under a constant load of about 130MPa [32]. The use of additional mechanical components may affect the overall performance of the SMA element, leading to friction which could influence the final functional parameters of the device. As opposite, the helical spring shape guarantees high strokes without the use of any further mechanical part but fairly small forces can be attained especially when embedded in miniature devices.

Hence, straight and helical spring conformations represent two opposite limits in the force versus stroke plane. In order to answer both to the need of stroke and force between these two limits, new SMA geometries should be studied.

In a recent work, a new SMA conformation has been proposed [33]; it consists in a planar wavy formed NiTi wire, named snake-like arrangement. To understand the mechanical performance of this unusual conformation as respect to other shapes, three NiTi samples with different geometry, but with identical elemental composition, thermal history and power consumption were tested by means of a standard tensile test. In this investigation the NiTi wire was formed to have the straight conformation, the helical spring and the snake-like arrangements, and austenite and martensite mechanical responses were assessed separately. As can be seen in Figure 8 the snake-like shape has a mechanical behavior between the wire and the helical spring ones.

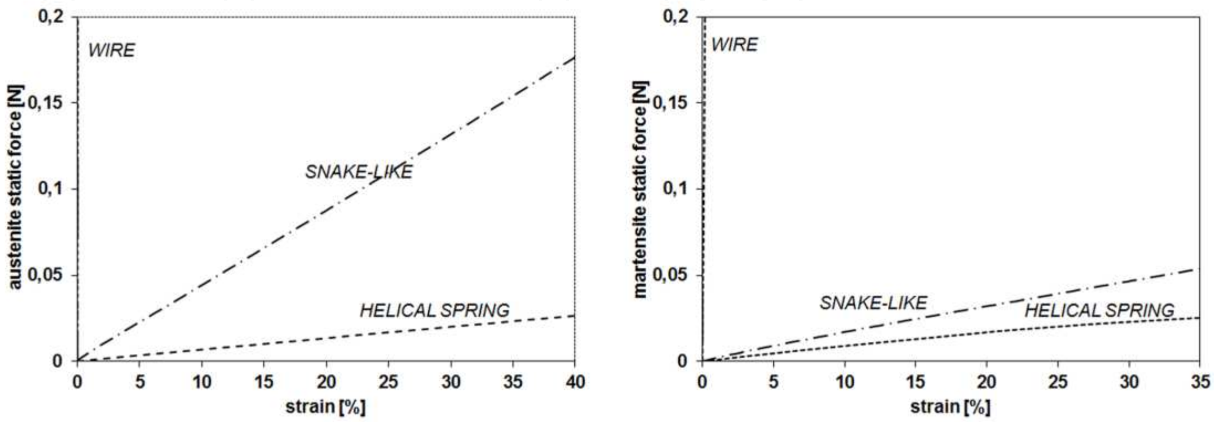

Figure 8. Comparison between austenite and martensite mechanical behavior of different NiTi wire geometries for actuators.

The snake-like conformation is characterized by four main parameters: the number of curvatures, N, the curvature radius, R, the distance between two consecutive curvatures, D, and the height, H. A snake-like specimen can be prepared by constraining a SMA wire in the snake-like arrangement by using a drilled aluminum bar and a series of nails; heating at high temperature is finally used to fix the shape. Figure 9 reports a snake-like sample prepared from a commercial NiTi wire having the diameter of 0.2mm, formed at 500°C during ten minutes and quenched in water at room temperature, with N=4, H=5.27mm±0.07mm, R=0.54mm±0.03mm and D=0.82mm±0.06mm.

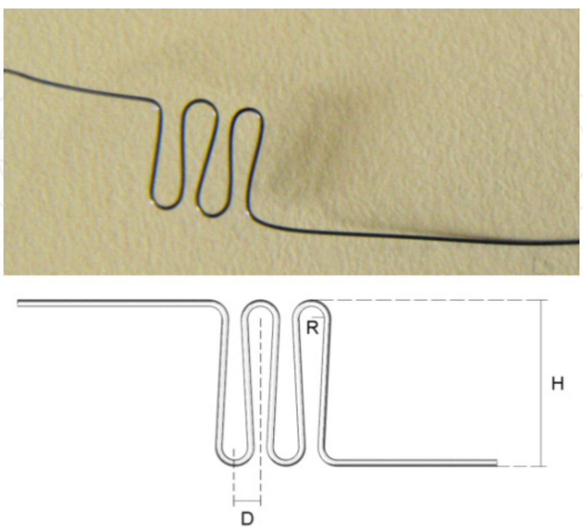

Figure 9. Snake-like NiTi wire with N=4, H=5.27mm±0.07mm, R=0.54mm±0.03mm and D=0.82mm±0.06mm.

As previously stated, during the ten minutes formation process the curved parts of the snake element are in contact with metal devices. This fact does not modify the calorimetric properties of the SMA element in all its length, as can be seen in Figure 10 where the overlapping of the DSC scans relative to the straight and the curved segments is clearly visible.

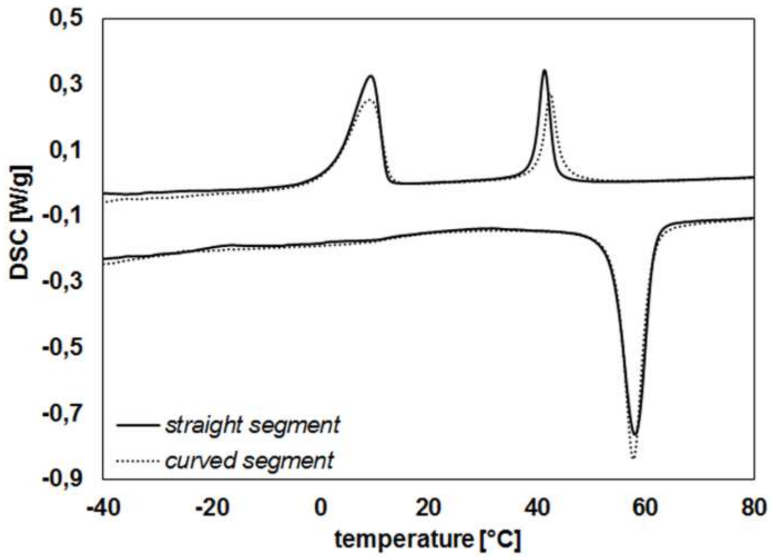

Figure 10. DSC scans of the straight and the curved part of the snake-like NiTi wire.

For small deformation values (see Figure 11), this snake-like shape shows an almost complete recovery of the deformation both for austenite and for martensite.

The relative higher output stroke performed by the snake-like NiTi wire as respect to the straight wire conformation is substantially due to the bend/unbend movement of the curvatures. In order to avoid plastic deformation and to achieve simultaneously a significant output stroke, the snake sample, formed as previously explained, should be stressed with a load near 0.1N, as forces lower and higher than 0.1N do not guarantee a proper functioning of this snake element: in fact, lower forces do not induce martensite formation, as opposite higher forces cause plastic deformations. As an example, in Figure 12 the curves derived from five thermal cycles of the snake-like NiTi sample under two constant loads, 0.1N and 0.2N is depicted. By comparing the two trends, it can be seen that in both cases the snake sample lose part of its shape recovery during cycling; this is much more visible for the specimen stressed with 0.2N.

Fatigue life was studied under the constant load of 0.1N; the snake-like sample was electrically activated with 0.6A with a maximum power consumption of 1W and a work frequency of 0.1Hz. Fracture takes place at the apex of that curvature most far from the applied load and from Figure 13 it can be observed that it occurs near the $7{,}5 \times 10^4$ cycle. The fractured section was analyzed through SEM observation, see the inset of Figure 13; it can be seen a region with the striation of the crack propagation departing from a nucleation site placed on the inner surface of the snake and a region characterized by dimples, typical of ductile materials.

After the cycling test, the DSC scan shows a feeble shifting of the transformation temperatures towards higher values; a better definition of the rhombohedral phase during heating is also visible (see Figure 14).

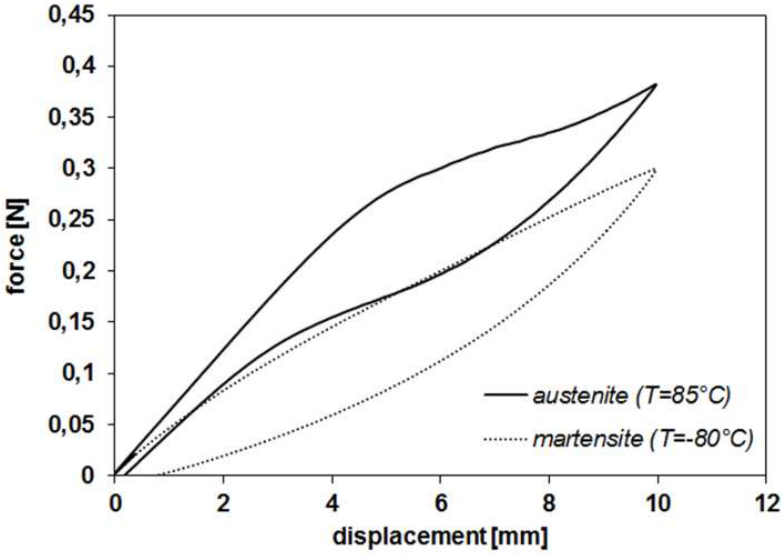

Figure 11. Force versus displacement of austenite and martensite of the snake-like NiTi wire.

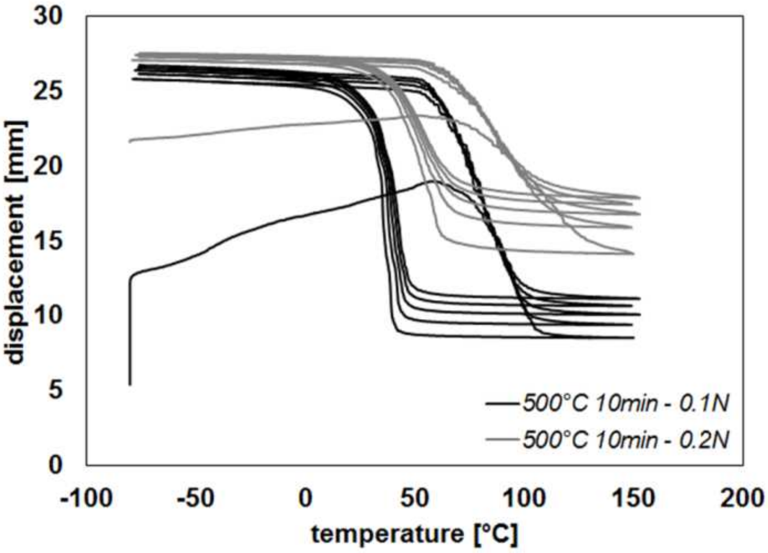

Figure 12. Hysteresis curves of the snake-like NiTi sample treated at 500°C for 10 minutes under 0.1N and 0.2N constant load.

When embedded in mini-modular device, the snake-like wire does not lose its mechanical performance. As an example, in Figure 15 a miniature rotational actuator composed by two mutual antagonist NiTi snake-like wire is reported [34]. The device exerts a stroke of about 120° under a constant torque of 0.1Nmm, as shown in Figure 16; it is activated by 0.6A with a maximum power consumption of 1W and a work frequency of 0.05Hz. Due to the particular construction, plastic deformation of the SMA element is prevented as the SMA elements never exceed 6mm of deformation.

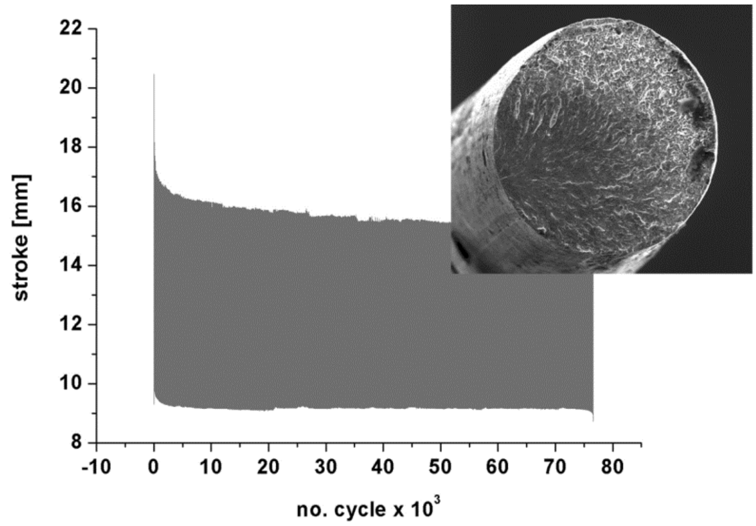

Figure 13. Snake-like NiTi sample fatigue test result under 0.1N load.

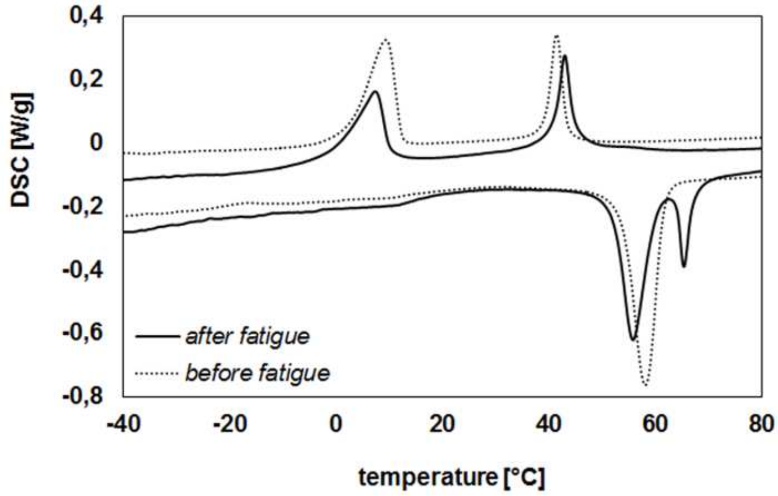

Figure 14. Snake-like NiTi sample DSC scan before and after the fatigue test

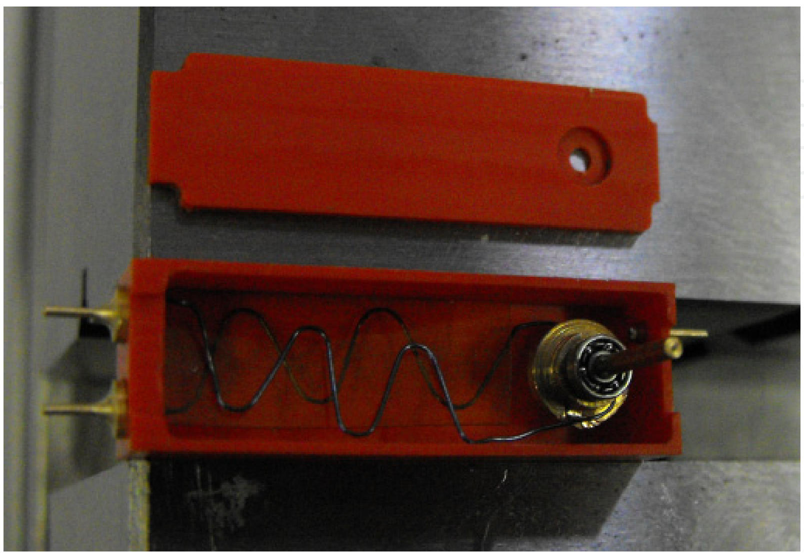

Figure 15. Mini rotational actuator activated by two antagonists snake-like NiTi wires.

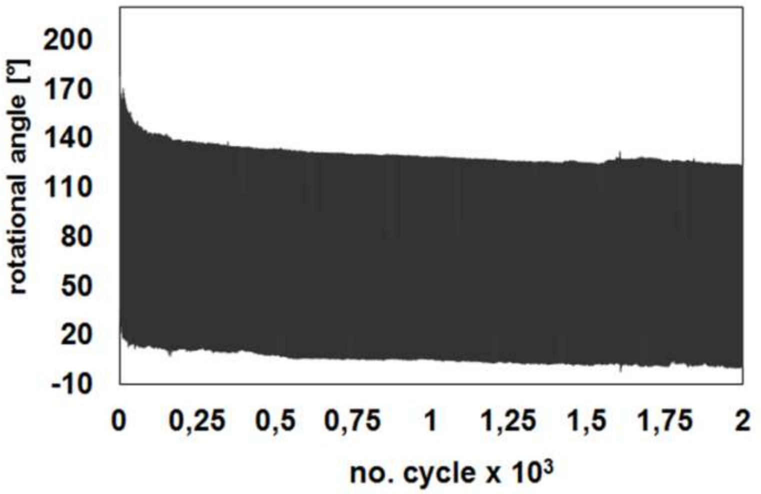

Figure 16. Fatigue test results of the mini rotational actuator under 0.1Nmm constant torque.

3.1. Micro snake-like shape memory alloy elements

In the last years the trend of miniaturization of components and products has been evidently introduced in several industrial fields, such as biomedical, electronics, aerospace and mechanics [35-36]. SMAs, as it already happens in biomedical applications [14,15,37-40], can be machined using laser machining with appreciated and high qualitative results [12]. The decision to investigate this method for the production of SMA actuators is considered an interesting topic because it shows some relevant advantages in comparison with other technologies, such as high productivity, high quality and repeatability, when applied in the industrial world.

Hence, the snake geometry can be easily scale down to the micro scale by the employment of laser technology with appreciated and high qualitative results. Because laser material processing is a thermal process, in which an heat source is used to remove a certain volume of material from the work piece, some thermal damages are evidently obtained, such as melted material, heat affected zone and oxides. To remove these defects, chemical etching and electro-chemical polishing have to be performed on the snake SMA samples [37,41]. Figure 17 depicts SEM images of the snake NiTi sample after laser, chemical etching and electro-chemical processes; top and bottom surfaces as well as snake sample section are shown. It can be seen that laser damages are mainly visible on the bottom surface and that the chemical etching remove the great part of defects. Moreover, a significant loss of mass and consequent reduction of the dimensions of the micro-snake can be evidently observed from SEM pictures due to the material removal of the post-processing. The snake NiTi sample geometry and calorimetric properties change after each process, as can be seen in Figure 18 and in Figure 19 respectively. In particular, the geometrical dimension are referred to a micro-snake obtained starting from a 120μm NiTi sheet. As concern the DSC data, it can be observed that the laser machining produces a refinement of the rhombohedral phase peak both on cooling and heating while the martensite peak barely change as respect to the unworked 120mm thick sheet, being almost spread and invisible. The laser process also yields a conspicuous diminution of the rhombohedral phase transformation temperatures and of the martensite starting temperature while the other characteristic transformation temperatures do not have an analogous variation being almost unchanged. Chemical etching and electro-polishing steps do not visibly alter any phase transformation temperature both on cooling and on heating, even if some little change due probably to the hydrogen introduction in the chemical process, is visible [45,46].

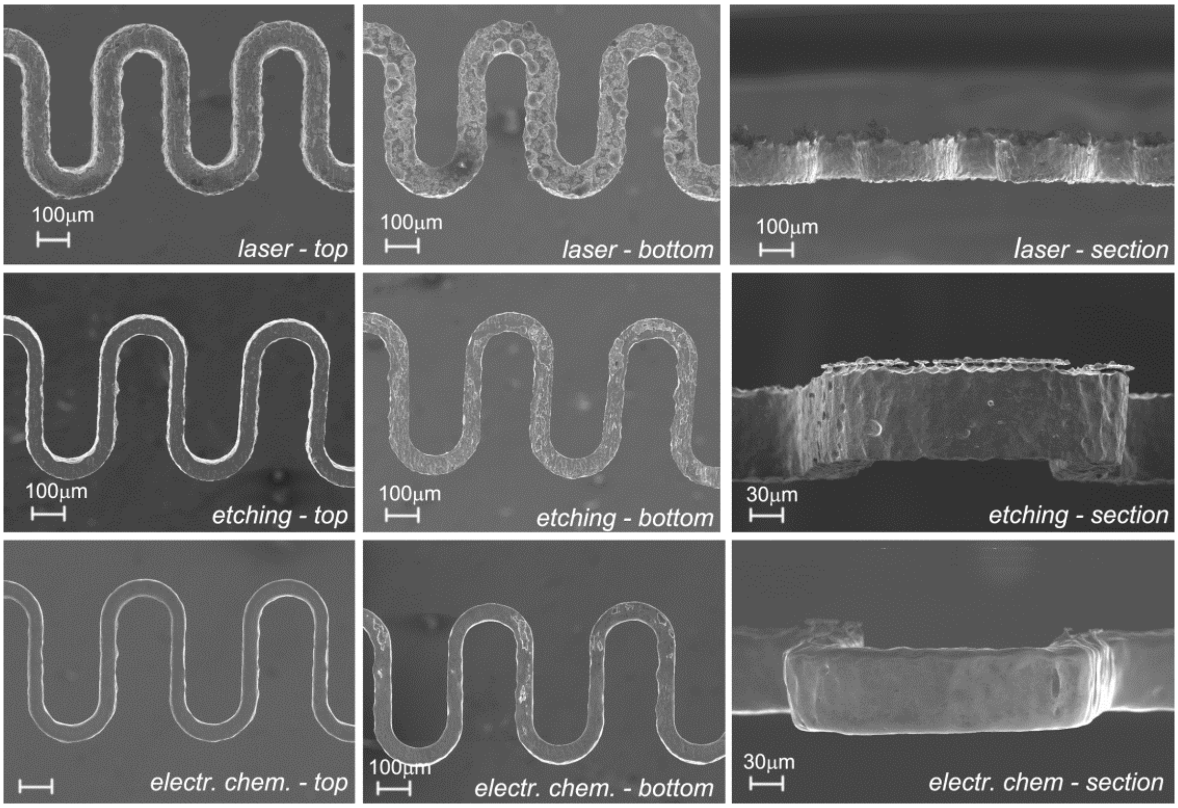

Figure 17. SEM images of the snake NiTi sample surfaces and section after laser, chemical etching and electro-polishing processes.

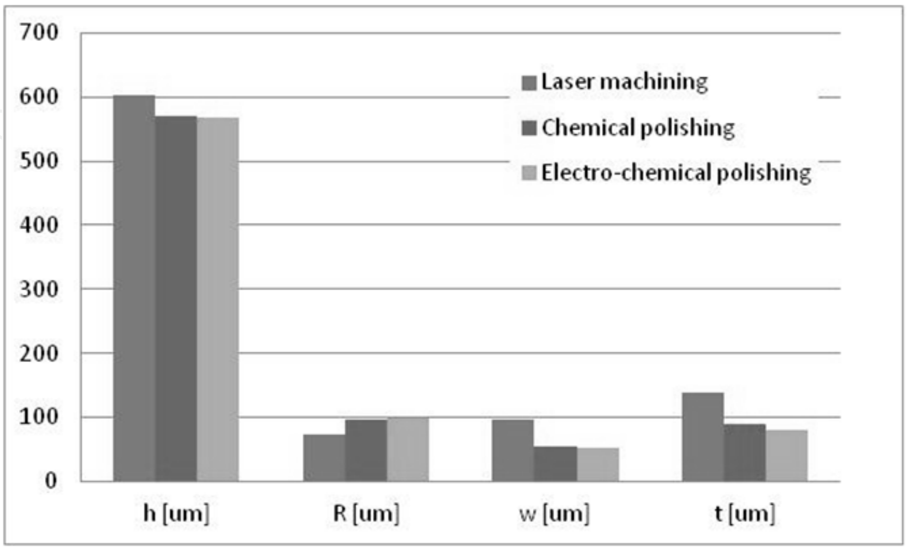

Figure 18. Variation of the geometrical parameters of the micro-snake during the fabrication process (h: high, R: radius of curvatures, w: width, t: thickness).

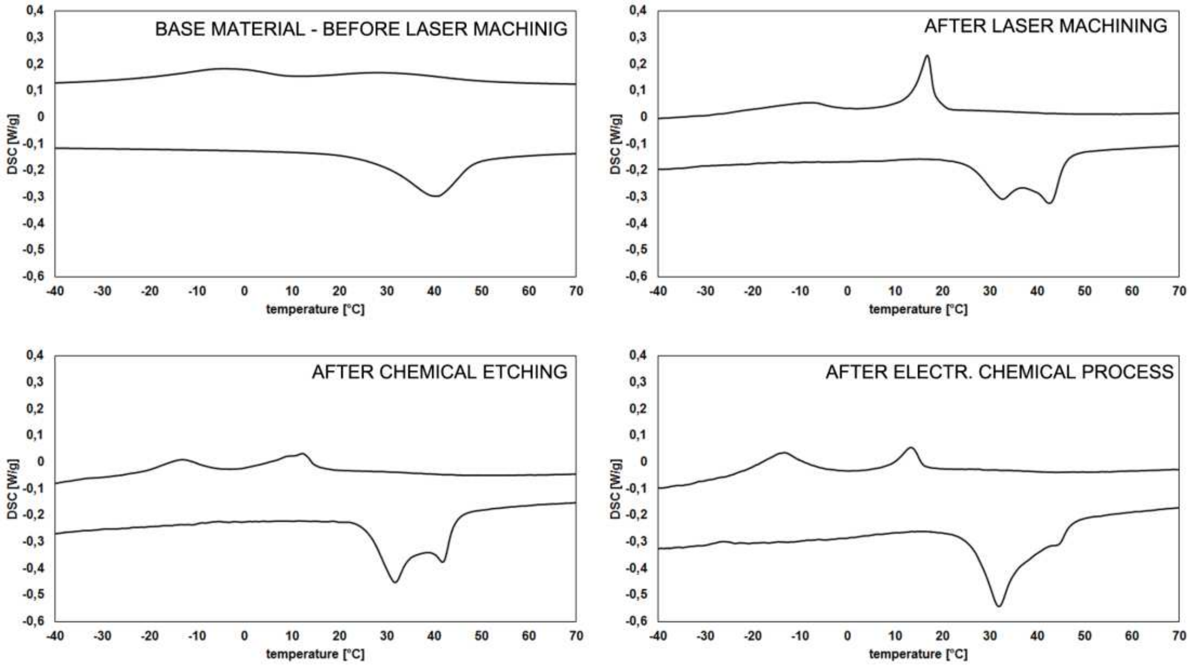

Figure 19. DSC scans before laser machining and in correspondence of each fabrication process.

The fabrication process previously described can be used to produce snake SMA sample of different length. As an example, Figure 20 depicts the SEM image of a micro-snake NiTi sample with 19 curvatures (i.e. 3.8mm of length) obtained starting from a 120μm NiTi sheet treated at 400°C for 15 minutes and quenched in water.

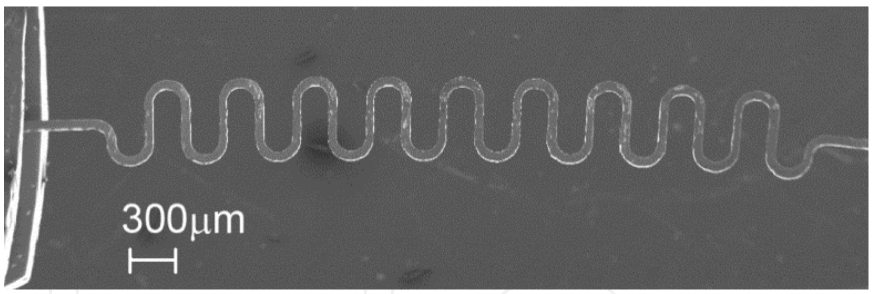

Figure 20. SEM image of a micro-snake NiTi sample obtained starting from a 120μm NiTi sheet.

Strain-recovery and thermo-mechanical cycling tests demonstrate the high performance of this micro-snake sample. As an example, under the constant load of 16mN, it reaches about 40% of recovery with a cycling stabilization within few hundreds of cycles, when heated by electrical current (130mA) with a maximum power consumption of 0.3W and a frequency of 0.15Hz.

4. Conclusions

In this work, new developments on SMA actuators in the mini/micro scale are presented: the attention was focused on straight NiTi thin wires and mini/micro snake-like NiTi samples.

Several working parameters have proved to strongly affect the functional and fatigue properties of SMA actuator, such as the electrical pulse performed to heat a wire, the different drawing procedures carried out to produce the wire or the wire arrangement into the device.

Then, the functional parameters of a snake-like NiTi wire demonstrate that this kind of geometry may be a good alternative to the most common geometries. It can generate a shape recovery in a very large range of deformation comparing to the straight SMA wire. This point is very beneficial for practical uses since the new proposed SMA conformation just occupies small space to generate the same displacement as the straight one, and it demonstrates to maintain its general mechanical performance when embedded in a mini-modular mechanical device. Finally, the presented fabrication process adopted for the manufacturing of micro-actuators looks to be very attractive (laser process can be performed on a large family of materials with high repeatability). The thermo-mechanical behavior of the micro-snake actuator can be considered interesting in the range of low applied load values with a good cycling stability.

Author details

Adelaide Nespoli*, Carlo Alberto Biffi, Riccardo Casati,
Francesca Passaretti, Ausonio Tuissi and Elena Villa
Consiglio Nazionale delle Ricerche, Istituto per l'Energetica e le Interfasi (CNR-IENI), Lecco, Italy

Acknowledgement

Authors would like to thank Prof. Barbara Previtali, head of Sitec-Laboratory for Industrial Laser Applications of Mechanical Department of Politecnico di Milano, for her precious support on the laser processing.

5. References

[1] Kazuhiro Otsuka, Clarence M Wayman (1998) ShapeMemoryMaterials. Cambridge University Press. 284 p.

[2] Hiroyasu Funakubo (1984) Shape memory alloys. London: Gordon and Breach Science Publishers.

[3] Miller DA, Lagoudas DC (2001) Influence of cold work and heat treatment on the shape memory effect and plastic strain development of NiTi. Mater. sci. eng. A. 308:161–75.

[4] Fukuda T, Kakeshita T, Kitayama M, Saburi T (1995) Effect of aging on martensitic transformation in a shape memory Ti–40.5Ni–10Cu alloy. J. phys. IV. 5:717–22.

[5] Degeratu S, Rotaru P, ManoleaGh, Manolea HO, Rotaru A (2009) Thermal characteristics of Ni–Ti SMA (shape memory alloy) actuators. J. therm. anal. calorim. 97:695–700.

[6] Villa E, Arnaboldi S, Tuissi A, Giacomelli M, Turco E (2009) Mechanical analysis of hybrid textile composites with NiTi wires. J. mater. eng. perform. 18(5–6):517–21.

* Corresponding Author

[7] Mineta T, Mitsui T, Watanabe Y, Kobayashi S, Haga Y, Esashi M (2001) Batch fabricated flat meandering shape memory alloy actuator for active catheter. Sens. actuators A. 88:112–20.

[8] Mineta T, Mitsui T, Watanabe Y, Kobayashi S, Haga Y, Esashi M (2002) An active guide with shape memory alloy bending actuator fabricated by room temperature process. Sens.actuators A. 97–98:632–7.

[9] Kohl M, Krevet B, Just E (2002) SMA microgripper system. Sens. and actuators A. 97-98:646-652.

[10] Leester-Schadel M, Hoxhold B, Lesche C, Demming S, Buttgenbach S (2008) Micro actuators on the basis of thin SMA foils. Microsyst. technol.14:697-704.

[11] John F.Ready, Dave F. Larson (2001) LIA Handbook of Laser Materials Processing. Laser Institute of America, Magnolia Publishing, Inc. p715.

[12] Dubey AK, Yadava V (2008) Laser beam machining—A review. Int. J. mac. tools manuf. 48:609–628.

[13] Gower MC (2000) Industrial applications of laser micromachining. Opt. Express 7:56-57

[14] Li C, Nikumb S, Wong F (2006) An optimal process of femtosecond laser cutting of NiTi shape memory alloy for fabrication of miniature devices. Opt. and lasers in eng. 44:1078–1087

[15] Momma C, Knop U, Nolte S (1999) Laser cutting of slotted tube coronary stents –state of the art and future developments. Prog. in biomed. res. 39-44.

[16] Buttgenbach S, Butefish S, Leester-Schadel M, Wogersien A (2001) Shape Memory Microactuators. Microsys. technol. 7:165-170.

[17] Meijer J, Du K, Gillner A, Hoffmann D, Kovalenko VS, Masuzawa T, Ostendorf A, Poprawe R, Schulz W (2002) Laser machining by short and ultrashort pulses, state of the art and new opportunities in the age of the photons, CIRP Ann. Manufact. Technol. 51:531-550.

[18] Saikrishna CN, Ramaiah KV, Allam Prabhu S, Bhaumik SK (2009) On stability of NiTi wire during thermo-mechanical cycling. Bull. mater. sci. 32:343–352

[19] Zanotti C, Giuliani P, Arnaboldi S, Tuissi A (2010) Analysis of wire position and operating conditions of functioning of NiTi wires for shape memory actuators. Proc. SMST 2010. 688-696.

[20] Frenzel J, George EP, Dlouhy A, Somsen CH, Wagner MFX, Eggeler G (2010) Influence of Ni on martensitic phase transformations in NiTi shape memory alloys. Actamater. 58:3444–3458.

[21] Casati R, Tuissi A, Belochapkine S, Dickinson C, Tofail SAM Thin NiTi wires with reduced thermal hysteresis for shape memory actuators. doi:10.1142/S1793604 7125000991250009

[22] Miller DA, Lagoudas DC (2001) Influence of cold work and heat treatment on the shape memory effect and plastic strain development of NiTi. Mat. Sci. Eng. A. 308:161-175.

[23] Todoroki T, Tamura H (1987) Effect of heat treatment after cold working on the phase transformation in TiNi alloy. Tran. of the jpn. Inst. of met. 28:83-94.

[24] Frick CP, Ortega AM, Tyber J, Maksound AEM, Maier HJ, Liu Y, Gall K (2005) Thermal processing of polycrystalline NiTi shape memory alloys. Mat. sci. eng. A. 405:34-49

[25] Contardo L, Guenin G (1990) Training and two way memory effect in Cu-Zn-Al alloy. Acta metall. mater. 38:1267-1272.
[26] http://www.cambridgemechatronics.com/
[27] Casati R, Tuissi A (2011) Effect of current pulses on fatigue of thin NiTi wires for shape memory actuators. Proc. SMST 2011. Submitted
[28] Wagner MFX, Dey SR, Gugel H, Frenzel J, Somsen Ch, Eggeler G (2010) Effect of low-temperature precipitation on the transformation characteristics of Ni-rich NiTi shape memory alloys during thermal cycling. Intermet. 18:1172-1179.
[29] Simon T, Kroger A, Somsen C, Dlouhy A, Eggeler G (2010) On the multiplication of dislocations during martensitic transformation in NiTi shape memory alloys. Acta mater. 58:1850-1860.
[30] Ibarra A, San Juan J, Bocanegra EH, Nò ML (2007) Evolution of microstructure and thermomechanical properties during superelastic compression cycling in Cu-Al-Ni single crystal. Acta Mater. 55:4789-4798.
[31] Nespoli A, Besseghini S, Pittaccio S, Villa E, Viscuso S (2010) The high potential of shape memory alloys in developing miniature mechanical devices: A review on shape memory alloy mini-actuators. Sens. and actuators A.158:149–160
[32] Jansen S, Breidert J, Welp EG (2004) Positioning actuator based on shape memory wires. Actuators 2004. 9th International Conference on New Actuators.
[33] Nespoli A, Villa E, Besseghini S (2011) Thermo-mechanical properties of snake-like NiTi wires and their use in miniature devices. J. therm.anal calorim. DOI 10.1007/s10973-011-1324-0
[34] Nespoli A, Bassani E, Besseghini S, Villa E (2010) Rotational mini-actuator activated by two antagonist shape memory alloy wires. Phis. Procedia 10:182-188
[35] Hsu T (2002) Miniaturization – A paradigm shift in advanced manufacturing and education. Proc. IEEE/ASME
[36] Feldmann K, Franke J, Schüßler F (2010) Development of micro assembly processes for further miniaturization in electronics production. CIRP Annals –Manufact. technol. 59:1–4
[37] Kathuria YP (2005) Laser microprocessing of metallic stent for medical therapy. J. of Mater. Process. Technol. 170:545-550
[38] Meng H, Liao J, Zhou Y, Zhang Q (2009) Laser micro-processing of cardiovascular stent with fiber laser cutting system.Opt. And laser technol. 41:300– 302
[39] Previtali B, Arnaboldi S, Bassani P, Biffi CA, Lecis N, Tuissi A, Carnevale M, LoConte A (2010) Microcutting of NiTiCu alloy with pulsed fiber laser.ISBN 978-0-7918-3877-8, Order No. I844CD
[40] BiffiC A, Bassani P, Tuissi A, Carnevale M, Lecis N, LoConte A, Previtali B (2011) Flexural Vibration Suppression of Glass Fiber/CuZnAl SMA Composite. Funct. Mater. Lett., DOI 10.1142/S1793604712500142
[41] Raval A, Choubey A, Engineer C, Kothwala D (2004) Development and assessment of 316LVM cardiovascular stents. Mater.sci. and eng. A.386:331–343.
[42] Kudesia SS, Solana P, Rodden W, Hand DP, Jones J (2005) Appropriate Regimes of Laser Drilling Models Containing Melt Eject Mechanisms. Journal of Laser Applications, 14:159-164.

[43] Rao BT, Kaul R, Tiwari P, Nath AK (2005) Inert gas cutting of titanium sheet with pulsed mode CO2 laser. Opt. and Lasers in Eng. 43:1330–1348
[44] Biffi CA, Lecis N, Previtali B, Vedani M, VimercatiG (2010) Fiber laser microdrilling and its effect on material microstructure. The int. j. of adv. manuf. Technol. 51:983-994
[45] Mazzolai FM, Biscarini A, Coluzzi B, Mazzolai G, Villa E, Tuissi A (2007) Low frequency internal friction of hydrogen-free and hydrogen-doped NiTi alloys. Acta mater.55:4243-425
[46] Biscarini A, Coluzzi B, Mazzolai G, Mazzolai FM, Tuissi A (2003) Mechanical spectroscopy of H-free and H-doped NiTiCu shape memory. J. of alloy and compd.356:669-672